Molecules **2007**, *3*, 907-916

molecules

ISSN 1420-3049

www.mdpi.org/molecules

Full Paper

Determination of the Three-dimensional Structure of Gynoside A in Solution using NMR and Molecular Modeling

Qian Li [1], Zhi-Hong Yao [2], Yan-Hong Shi [3], Xin Liu [1], Xin-Sheng Yao [2] and Wen-Cai Ye [1,2,*]

[1] Department of Phytochemistry, China Pharmaceutical University, Nanjing 210009, P. R. China; E-mails: kathylqnmr@hotmail.com; xinliuchina@sina.com.cn

[2] Institute of Traditional Chinese Medicine and Natural Products, Jinan University, Guangzhou 510632, P. R. China; E-mails: yaozhihong5198@yahoo.com.cn; yaoxinsheng@163.net

[3] Department of Analytical Chemistry, Shanghai Institute of Materia Medica, Shanghai Institutes for Biological Sciences, CAS, Shanghai 201203, P. R. China; E-mail: shi_yanhong@yahoo.com.cn

* Author to whom correspondence should be addressed. E-mail: chywc@yahoo.com.cn; Fax: +86-20-85221559

Received: 23 March 2007; in revised form: 5 April 2007 / Accepted: 18 April 2007 / Published: 30 April 2007

Abstract: The three-dimensional structure of Gynoside A, an ocotillone-type triterpenoid glycoside isolated from *Gynostemma pentaphyllum*, was determined in pyridine-d_5 and DMSO-d_6 solution through constrained molecular modeling using constraints derived from proton NMR spectra. The calculation yielded well-defined global minima. Except for some quantitative details the overall structure of Gynoside A in pyridine-d_5 shared many common features with that in DMSO-d_6. The structure in pyridine-d_5 had lower energies than that in DMSO-d_6 solution.

Keywords: NMR, Gynoside A, triterpenoid glycoside, molecular modeling.

Introduction

Triterpenoid glycosides had been extensively studied because of their widespread occurrence in plants and a varied bioactivities, such as antitumor, anti-inflammatory, cholesterol level lowering, etc [1-4]. Structurally, triterpenoid glycosides have both aglycone and sugar-chains, which are normally appended to the C-3 or/and C-28 positions of the aglycone, respectively. Many research indicated that

the bioactivities of triterpeonid glycoside was not only related to aglycone itself, but also to the characters of sugar-chain, such as the amount and category of sugars, the biding site and sequence of sugar-chain, etc. Few of the three-dimensional structures of saponins were reported due to the difficulty suitable single crystals for X-ray diffraction analysis. The structure of (20*S*,24*S*)-20,24-epoxy-12,25-dihydroxy-dammaran-3-yl-*O*-β-D-glucopyranosyl(1→2)-β-D-xylopyranoside (Gynoside A, Figure 1), an ocotillone-type triterpenoid glycoside isolated from *Gynostemma pentaphyllum*, determined by X-ray diffraction has been reported [5]. In this paper, the three-dimensional structures of Gynoside A in pyridine-d_5 and DMSO-d_6 were determined via constrained molecular modeling using constraints derived from NMR spectra, which can be used for determination of the fine detail of the structures such as the precise orientation of the sugar rings. A comparison of the single crystal and two solution-phase structures is presented here.

Figure 1.

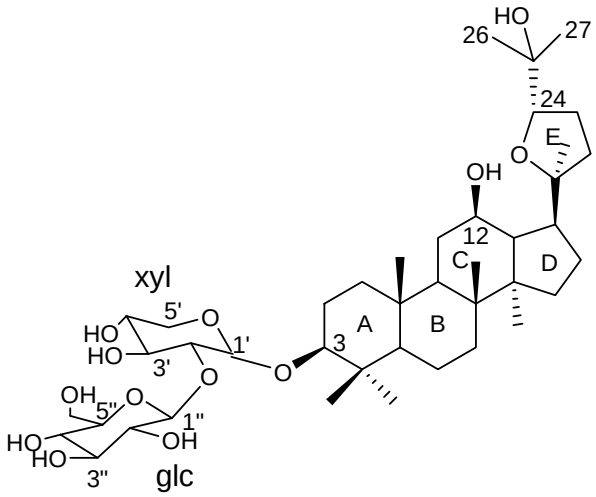

Results and Discussion

NMR assignments

The ^{1}H spin system identification and assignments were accomplished through COSY and TOCSY experiments. The chemical shifts of the corresponding carbons were directly assigned from the HSQC experiment after the protons had been assigned. The quaternary carbon atoms were identified by HMBC. The assignments of ^{1}H- and ^{13}C-NMR resonances in the two solutions are listed in Table 1.

Table 1. NMR data of Gynoside A .

No.	Pyridine-d_5		DMSO-d_6	
	δ (^{13}C)	δ (^{1}H)	δ (^{13}C)	δ (^{1}H)
1	39.8	1.68	38.5	1.60 (He), 0.93 (Ha)
2	27.3	2.21 (He), 1.93 (Ha)	25.9	1.75 (He), 1.60 (Ha)
3	89.2	3.28	87.9	3.02

Table 1. Cont.

No.	Pyridine-d_5		DMSO-d_6	
	δ (^{13}C)	δ (^{1}H)	δ (^{13}C)	δ (^{1}H)
4	40.2			
5	57.0	0.75	55.6	0.73
6	19.0	1.54 (He), 1.42 (Ha)	17.7	1.47 (He), 1.40 (Ha)
7	35.6	1.40 (He), 1.25 (Ha)	34.3	1.40 (He), 1.22 (Ha)
8	40.5			
9	51.0	1.52	49.5	1.40
10	37.5		36.3	
11	33.0	1.42 (He), 2.15 (Ha)	31.8	1.75
12	71.2	3.77	69.5	3.34
13	50.0	1.85	48.4	1.58
14	52.8		51.5	
15	33.2	1.54 (He), 1.02 (Ha)	31.8	1.47 (He), 1.02 (Ha)
16	29.1	1.87 (He), 1.27 (Ha)	27.7	1.85 (He), 1.29 (Ha)
17	49.9	2.31	48.4	2.09
18	16.1	1.04	15.1	0.95
19	17.1	0.90	16.0	0.82
20	87.5		86.1	
21	29.5	1.33	28.3	1.17
22	32.7	2.03 (He),1.71(Ha)	31.5	1.83
23	26.2	2.21(He),1.96 (Ha)	24.9	1.82
24	88.9	4.16	87.0	3.69
25	70.4		69.2	
26	27.4	1.47	26.4	1.00
27	27.0	1.33	25.5	1.03
28	28.5	1.30	27.3	0.98
29	17.0	1.13	15.7	0.75
30	18.5	0.93	17.6	0.85
Xyl 1’	106.1	4.86	104.2	4.28
2’	83.8	4.21	81.1	3.35
3’	78.5	4.26	76.0	3.34
4’	71.4	4.17	69.3	3.34
5’	67.2	4.31 (He), 3.70 (Ha)	65.1	3.69 (He), 3.07 (Ha)
Glc 1’’	106.6	5.37	103.8	4.44
2’’	77.5	4.11	75.1	3.02
3’’	78.5	4.26	76.0	3.16
4’’	72.1	4.37	69.3	3.15
5’’	78.8	3.95	76.7	3.06
6’’	63.1	4.50	60.8	3.63 (He), 3.51 (Ha)

NMR constraints

Based on the isolated spin-pair approximation, the interproton distance for the pair H_k-H_l can be obtained from the equation $r_{kl}=r_{ij}(\sigma_{ij}/\sigma_{kl})^{1/6}$, where σ_{ij} and σ_{kl} are the cross-relaxation rates for unknown and calibration distances, respectively [6,7]. In this study, the distance restraints were obtained from the ROESY spectrum with a mixing time of 250 ms. ROE volumes were integrated with Sparky [8]. The 1.78Å distance between the germinal protons at H-6 of the aglycone was used as a reference. Although the intensity of ROESY cross peaks depends strongly on distance, there is a weak dependence on the vibration degrees of freedom of the molecule, especially for large-amplitude, low-frequency normal modes. Consequently, the distance calculated from the intensities are normally not treated as precise, well-determined numbers, but instead converted to upper bounds. The ROE cross peaks were classed as strong, medium, and weak, based on the distance (<3.0 Å for strong, <4.0 Å for medium and <5.0 Å for weak). The following sorting algorithm was used for the pairs of protons sugar ring: if the calculated interproton distance between sequential protons was 3.0 Å or less, the upper bound of 3.0 Å was assigned. The distance between pairs of protons separated by more than three bonds or on separated groups was treated as medium or long rang and the upper bound of 4.0 Å was applied irrespective of the calculated distance [9-11].

Methyl groups required an additional but necessary adjustment that diminishes their value in the determination of the structure. The distance between a methylene or methane proton and a methyl proton was converted to a proton-carbon bond using the above rules, and 1.0 Å was added to the bond [11, 12].

Scalar vicinal proton-proton coupling constants of the sugar residues (Table 2) could also be useful in constraining the structure, which is invaluable in defining the conformation. Large proton couplings (>8.5Hz) indicated a torsional angle close to an *anti* conformation (in the range of 180±30°), and the upper bounds in the distance between the coupled protons was set to 3.08Å. Small coupling protons (<2Hz) indicated a torsional angle close to a *gauche* conformation and the upper bounds was set to 2.77Å [12].

Table 2. Vicinal proton-proton coupling constant (Hz) yielding torsional constraints on the structure.

Coupled protons (A-X-Y-B)	^3J(A,B)	
	in pyridine-d_5	in DMSO-d_6
1'H-1'C-2'C-2'H	6.7	6.1
4'H-4'C-5'C-5'He	4.9	4.5
4'H-4'C-5'C-5'Ha	10.5	9.6
1"H-1"C-2"C-2"H	7.6	8.5
2"H-2"C-3"C-3"H	8.2	8.0
3"H-3"C-4"C-4"H	8.9	8.4
4"H-4"C-5"C-5"H	9.4	9.4
5"H-5"C-6"C-6"Ha	3.5	4.6
5"H-5"C-6"C-6"He	3.5	4.6

Structural results

47 NOE-derived distance constraints were used for the DMSO-d_6 and 33 for the pyridine-d_5 solution work. due to the fact that the hydroxyl proton signals of sugar rings can be distinguished in DMSO-d_6 solution (Figure 2). After calculation, 10 minimum energy structures among the last 100 ps were extracted and optimized by the conjugate-gradient method. The results are given in Table 3. All of the structures satisfied the distance constraint criteria with energies in the 186.2-191.5 kcal mol^{-1} range (1 kcal=4.184 kJ) in pyridine-d_5 and 203.8-207.9 kcal mol^{-1} for DMSO-d_6. The average root mean square deviation (rmsd) values for the mean structure in pyridine-d_5 and DMSO-d_6 were 0.837 and 0.521 Å, respectively. Obviously, the structure in pyridine-d_5 had lower energies than that in DMSO-d_6. The two global minimum energy conformations are displayed in Figure 3.

Figure 2. Expanded ROESY spectrum of Gynoside A in DMSO-d_6 at 300K (Mixing time, 250 ms). The exchange between the hydroxyl protons was manifested by positive cross peaks).

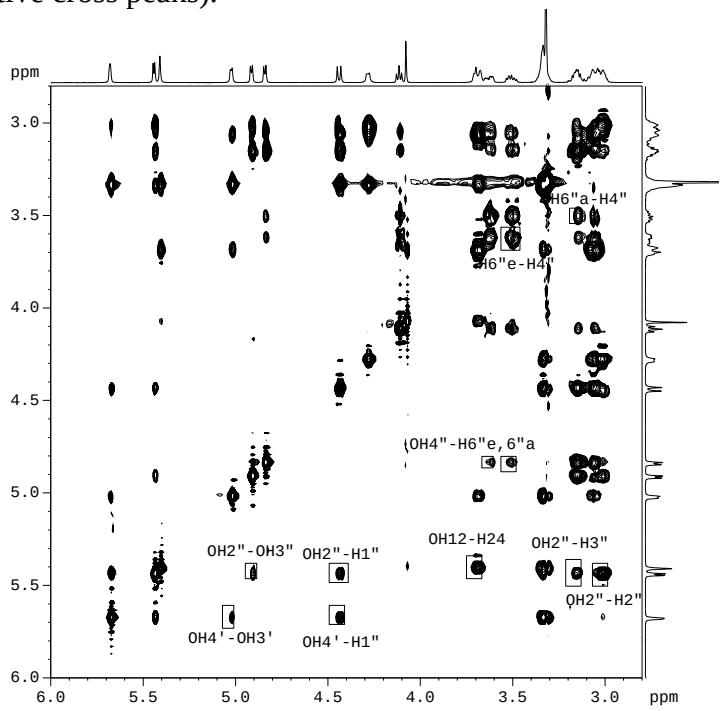

Table 3. Distance constraints in the structure of Gynoside A determined from the ROESY spectrum in pyridine-d_5 and DMSO-d_6.

Atom A-Atom B	Pyridine-d_5	DMSO-d_6	Atom A-Atom B	Pyridine-d_5	DMSO-d_6
$H_{5''}$—$H_{6''}$	3	-	H_3—C_{28}	4	4
$H_{5''}$—$H_{1''}$	4	-	H_3—C_{29}	5	-
$H_{1''}$—C_{29}	5	5	H_5—C_{28}	5	-
$H_{1'}$—H_2	4	-	$H_{5''}$—C_{29}	5	-
$H_{1'}$—H_3	4	-	$H_{6''}$—C_{29}	5	-
$H_{1'}$—$H_{3'}$		4	H_{12}—H_{11}	3	3
$H_{1'}$—$H_{5'}$	4	-	H_{12}—H_{17}	3	3

Table 3. Cont.

$H_{1'}$—C_{28}	5	5	H_{12}—C_{30}	5	5
H_3—H_5	3	-	OH_{12}—H_{13}	3	3
H_3—H_{19}	3	-	OH_{12}—H_{12}	3	3
OH_{12}—H_{17}	4	3	OH_{12}—H_{11}	4	
OH_{12}—H_{24}	3	3	OH_{12}—C_{26}	5	-
OH_{12}—C_{21}	-	5	OH_{12}—C_{27}	-	5
OH_{25}—C_{26}	4	5	OH_{25}—C_{27}	5	-
OH_{25}-C_{21}	-	5	OH_{25}—C_{24}	4	4
$OH_{2''}$—$H_{1''}$	-	4	$H_{1''}$—$H_{4''}$	-	4
$OH_{2''}$—$H_{3''}$	4	4	$OH_{2''}$—$H_{2''}$	-	3
$OH_{3''}$—$H_{2''}$		4	$OH_{2''}$—$OH_{3''}$	-	4
$OH_{4''}$—$H_{3''}$		4	$OH_{3''}$—$H_{3''}$	3	3
H_3—H_2	-	3	$H_{1''}$—$H_{5''}$		4
$OH_{3'}$—$H_{5'}$	-	4	$OH_{4''}$—$H_{6''a}$	-	4
$OH_{3'}$—$H_{2'}$		4	$OH_{4''}$—$H_{6''e}$	-	4
$OH_{3'}$—$H_{3'}$	3		$H_{1''}$—$H_{2'}$		4
$OH_{4'}$—$H_{1''}$	5	4	$OH_{6''}$—$H_{6''a}$	-	3
$OH_{4'}$—$OH_{3'}$	-	4	$OH_{6''}$—$H_{6''e}$	-	3
$H_{6''a}$—$H_{4''}$	-	4	H_{12}—H_9	-	3
$H_{6''e}$—$H_{4''}$	-	4	H_{17}—C_{21}	5	5
H_{17}—H_{22}	-	3	H_{17}—C_{30}	5	5
H_{22a}—C_{21}	-	4	H_{22e}—C_{21}	-	4
H_{24}—H_{13}	-	3	H_{24}—H_{22e}	-	3
H_{24}—C_{27}	-	4	H_{24}—C_{26}	5	5

The overall backbone structure of Gynoside A in pyridine-d_5 shared several features in common with that of DMSO-d_6. In pyridine-d_5 solution, the A, Band C rings of Gynoside A adopted chair conformations (Figure 3). Both rings D and E, which are 5-membered rings, appear to exist in an envelope conformation. The A, B, C and D rings were approximately parallel, and the E ring was perpendicular to the plane of A, B, C and D ring. In DMSO-d_6 solution, the general topology of the conformation was similar to that of pyridine-d_5.

Our calculations yielded a $^4C_1$ conformation for the xylose and glucose units in pyridine-d_5 and DMSO-d_6 solution, respectively. All of the hydrogen protons on the xylose ring were axial except one of the 5'-H with 1'-H, 3'-H, and 5'a-H on one side and 2'-H, 4'-H on the other side. The 10.5 Hz value of ^3J(4', 5'a) indicated that 4'-H and 5'a-H were diaxial. Moderately strong ROEs correlations between pairs of 1'-H and 5'a-H in DMSO-d_6, and between 1'-H and 3'-H in pyridine-d_5 were observed.

Figure 3. The two global minimum energy conformations of Gynoside A (I in pyridine-d_5; II in DMSO-d_6).

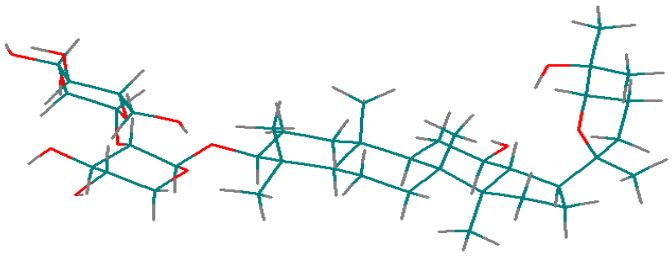

I

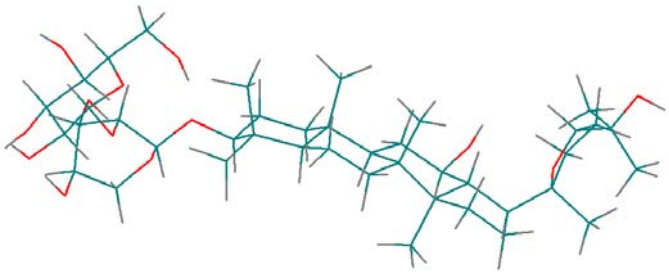

II

All of these data support the chair conformation of xylose ring. For the glucose ring, all of the ethane hydrogens on the pyranose ring were axial. The large coupling constants ^3J (2", 3"), ^3J (3", 4") and ^3J (3", 4") indicated the anti orientation of the interprotons pairs. Moderately strong ROEs correlations between pairs of 5" and 1", OH-2" and 3" in pyridine-d_5, and OH-2" and 1", OH-2" and 3", OH-3" and 2", OH-4" and 3" in DMSO-d_6 were observed, which support the chair conformation of glucose ring.

The xylose unit was parallel to the plane of the aglycone. The glucose residue was pointing up to the A ring of the aglycone in both solvents. The torsional angles defining orientation of the aglycone and the two sugar residues are listed in Table 4.

Table 4. Torsional angles (°) for the orientation of aglycone and sugar units.

Torsional angle	Pyridine-d_5	DMSO-d_6
C_3-C_4-C_5-C_{10}	50.4±0.9	53.1±1.6
C_3-C_4-C_5-C_6	183.5±1.0	188.4±1.4
C_4-C_5-C_6-C_7	163.8±1.7	161.2±2.2
C_4-C_5-C_{10}-C_9	191.47±1.3	193.3±1.5
C_6-C_7-C_8-C_{14}	193.0±1.9	192.3±1.6
C_6-C_7-C_8-C_9	312.0±1.7	311.3±1.7
C_7-C_8-C_9-C_{10}	47.3±2.0	47.9±1.7
C_7-C_8-C_9-C_{11}	185.9±2.3	185.9±0.6
C_7-C_8-C_{14}-C_{13}	177.1±1.5	176.9±0.6
C_7-C_8-C_{14}-C_{15}	289.7±2.5	286.8±1.2

Table 4. Cont.

C_8-C_9-C_{11}-C_{12}	50.7±2.6	52.7±0.5
C_8-C_{14}-C_{13}-C_{17}	165.4±2.0	161.9±0.8
C_8-C_{14}-C_{15}-C_{16}	201.0±3.0	199.5±0.5
C_{16}-C_{17}-C_{20}-O	194.5±2.2	190.3±1.0
C_{16}-C_{17}-C_{20}-C_{22}	306.2±2.8	306.7±1.1
C_{15}-C_{16}-C_{17}-C_{20}	120.1±2.9	117.1±1.1
C_2-C_3-O-$C_{1'}$	135.9±3.5	145.0±1.5
C_3-O-$C_{1'}$-$C_{2''}$	187.4±2.4	146.1±2.0
$C_{1'}$-$C_{2'}$-O-$C_{1''}$	113.5±2.3	154.1±1.2
$C_{2'}$-O-$C_{1''}$-$C_{2''}$	91.2±1.5	155.7±2.4

When comparing the X-ray structure with that derived from NMR, the general topology was maintained in the structure of solvent, except for some differences in the quantitative details [5, 18]. The A, B and C rings of Gynoside A adopted chair conformations and rings D and E displayed envelope conformations. Both xylose and glucose units adopt $^4C_1$ conformation which is identical with that of solution.

Taking these observations into account, the structure in pyridine-d_5 had lower energies than that in DMSO-d_6. The general topology of the conformation was maintained in both solvents and crystal structure, so we could reasonably assume that the simulation of rigid structure of the triterpenoid glycoside with restraints obtained from NMR in two different solvents gives a good picture of the solution-state conformation, as well as that of the solid-state one.

Experimental

General

Gynoside A was isolated from the leaves of *Gynostemma pentaphyllum*. About 10 mg of Gynoside A was dissolved in pyridine-d_5 and DMSO-d_6 (0.5 mL), respectively. The solvent and TMS signals were used as references for the chemical shifts. The samples were prepared by bubbling dry nitrogen through the solutions for 30 min. in order to ensure the removal of oxygen. All NMR experiments were performed at 300K on a BRUKER AV400 spectrometer equipped with a 5 mm gradient inverse broadband probe. 1D ^{1}H- and ^{13}C-NMR (BB and DEPT-135) measurements were obtained using standard methods. For all the 2D experiments, spectral widths of 4,000 and 20,000 Hz were used for the ^{1}H and ^{13}C dimensions, respectively. ROESY experiments were carried out with mixing times of 100, 200, 250, 300 and 400 ms. Chemical shift (δ values) were expressed in ppm and coupling constants (*J*) in Hz.

All the calculations were performed with HyperChem software (evaluation version 7.0) on a Intel® Pentium® processor 1.70 GHz computer using the MM+ force field. The starting structures were built using the model builder program in HyperChem. The molecule first underwent conjugate gradient minimization by the Polak-Ribiere method to remove any high-energy contacts.

MD simulations [13-17] were carried out by weak coupling in a temperature bath with a relaxation time of 100fs. No cutoff distance was used for all possible interactions. The electrostatic interactions were applied with a force constant of 7 kcal $mol^{-1}Å^{-2}$. To avoid trapping structures in local minima, simulated annealing method was employed: (1) a time of 10 ps to heat the system from 0 to 1000 K and then run 250 ps dynamic simulation. (2) a time of 10 ps to slowly cool to 300 K, and run 150 ps dynamic simulation, the trajectory structure was saved each 0.5 ps. (3) Ten low-energy conformations minimized with conjugate-graduate method were selected for the conformational analysis.

Acknowledgements

This work was supported by the National Natural Science Foundation of China (30472146), and the Project of Science and Technology of Guang-Dong province, China (2003A30909).

References and Notes

1. Cho, J.Y.; Yoo, E.S.; Cha, B.C.; Park, H.J; Rhee, M.H.; Han, Y.N. The inhibitory effect of triterpenoid glycosides originating from *Sanguisorba officinalis* on tissue factor activity and the production of TNF-α. *Planta Medica* **2006**, *72*, 1279-1284.
2. Popovich, D.G.; Kitts, D.D. Anticancer activity of ginseng and soy saponins. In *Nutrition and Cancer Prevention*; Awad, A.B.; Bradford, P.G., (Eds.); Taylor and Francis: Boca Raton, FL, **2006**; pp. 457-483.
3. Sugishita, E.; Amagaya, S.; Ogihara, Y. Structure-activity studies of some oleanane triterpenoid glycosides and their related compounds from the leaves of *Tetrapanax papyriferum* on antiinflammatory activities. *J. Pharmacobio-Dynam.* **1982**, *5*, 379-87.
4. Rao, A.V.; Gurfinkel, D.M. The bioactivity of saponins: triterpenoid and steroidal glycosides. *Drug Metab. Drug Interact*. **2000**, *17*, 211-235.
5. Liu, X.; Ye, W.C.; Mo, Z.Y.; Hsiao, W.L. Five New Ocotillone-Type Saponins from *Gynostemma pentaphyllum*. *J. Nat. Prod*. **2004**, *67*, 1147-1151.
6. Gao, J.H.; Shi, G.B.; Song, G.Q.; Shao, Y.; Zhou, B.N. Further NMR Investigation and Conformational Analysis of an Acylated Flavonol Glucorhamnoside. *Magn. Reson. Chem.* **1996**, *34*, 249-254.
7. Hudson, B.P.; Hudson; Barton, J.K. Solution Structure of a Metallointercalator Bound Site Specifically to DNA. *J. Am. Chem. Soc.* **1998**, *120*, 6877-6888.
8. Goddard, T.D.; Kneller, D.G. *SPARKY 3*; University of California: San Francisco, CA, **2006**.
9. Wüthrich, K.; Billeter, M.; Braun, W. Pseudo-structures for the 20 common amino acids for use in studies of protein conformations by measurements of intramolecular proton-proton distance constraints with nuclear magnetic resonance *J. Mol. Biol.* **1983**, *169*, 949-961.
10. Wüthrich, K. *NMR of Proteins and Nucleic Acids*; Wiley: New York, **1986**.
11. Steinmetz, W.E.; Sadowshy, J.D.; Rice, J.S.; Roberts, J.J.; Bui, Y.K. Determination of the aqueous-phase structure of 6-*O*-methylerythromycin from NMR constraints. *Magn. Reson. Chem.* **2001**, *39*, 163.

12. Steinmetz, W.E.; Sparrow, A.; Somsouk, M. Determination of the three-dimensional, solution-phase structure of the macrolide antibiotic oxolide in CD_2Cl_2 and D_2O from NMR constraints. *Magn. Reson. Chem.* **2005**, *43*, 16-20.
13. Liu, S.B.; Shi, Y.H.; Zhang, Q.W.; Song, G.Q. Conformational study of fosinopril sodium in solution using NMR and molecular modeling. *Magn. Reson. Chem.* **2003**, *41*, 609-614.
14. Shi, YH, Song, YL, Li, Q, Song, GQ. Binding affinity difference induced by the stereochemistry of the sulfoxide bridge of the cyclic peptide inhibitors of Grb2-SH2 domain: NMR studies for the structural origin. *Biochim. Biophys. Res. Commu.* **2005**, *330*, 1254-1261.
15. *Hyperchem 7.5 Master manual: Release 7 for Windows*; Hypercube Inc.: Florida, USA, **2002**.
16. Lins, L.; Brasseur, R.; Malaisse, W.J.; Biesemans, M.; Verheyden, P.; Willem, R. Importance of the hydrophobic energy: structural determination of a hypoglycemic drug of the meglitinide family by nuclear magnetic resonance and molecular modeling, *Biochem. Pharmacol.* **1996**, *52*, 1155-1168.
17. Gao, J.H.; Shi, G.B.; Song, G.Q.; Chen, K.X.; Ji, R.Y. Conformational studies of Asterin B and C in solution by NMR. II. Conformational analysis by NMR and molecular dynamic simulations. *Acta Chim. Sin*. **1996**, *54*, 702-708.
18. Crystallographic data for the compound Gynoside A reported in this paper have been deposited with the Cambridge Crystallographic Data Center and allocated the deposition number CCDC 200550. Copies of the data can be obtained, free of charge, on application to CCDC, 12 Union Road, Cambridge CB2 1EZ, UK [fax: +44(0)-1223-336033 or e-mail:deposit@ccdc.cam.ac.uk]

Sample Availability: Small samples (a few milligrams) of Gynoside A are available from the authors.